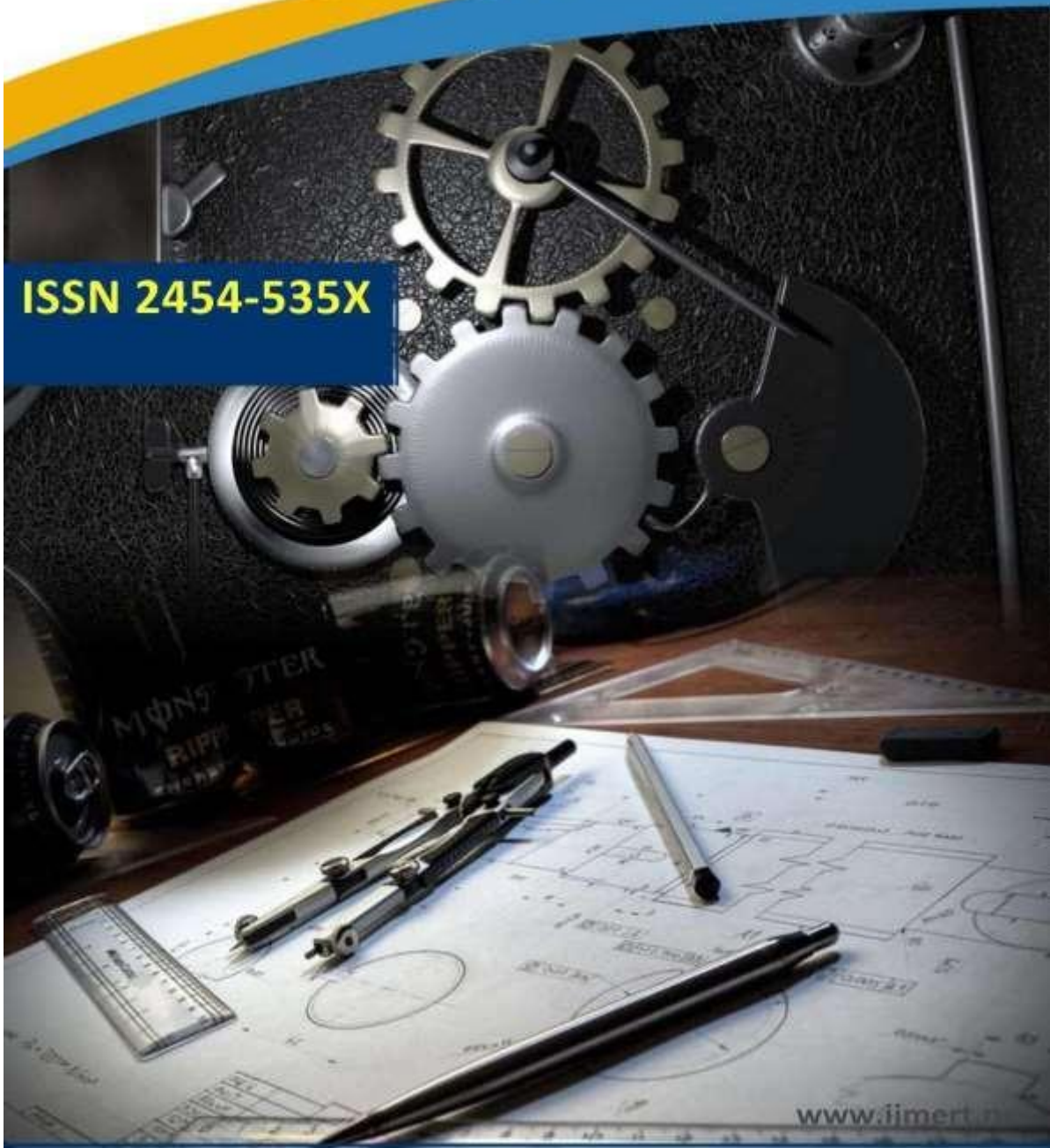




# International Journal of Mechanical Engineering Research and Technology

**ISSN 2454-535X**



[www.ijmert.net](http://www.ijmert.net)

**Email ID: [info.ijmert@gmail.com](mailto:info.ijmert@gmail.com) or [editor@ijmert.net](mailto:editor@ijmert.net)**

## Application of Inkjet Coating Printer to Assess MEA Cell Performance for PEFC

K. Monika\* & K. Sampadha

**ABSTRACT:** This research assesses the efficiency of membrane electrode assembly (MEA) utilized for Polymer Electrode Fuel Cell (PEFC) created by inkjet coating printer and suggests a new approach for manufacturing catalyst layers using this printer. In general, the high viscosity catalyst slurry for the doctor blade approach could not be directly applied to the inkjet printer. As a result, the solvent was added to this slurry to create the catalyst ink with the proper viscosity for the inkjet coating printer. Furthermore, we used a vacuum stirrer mill and ultrasonic wave crusher to increase the dispersibility of Pt because this catalyst ink has a low viscosity. As a result, the inkjet printer used this new catalyst ink to build the catalyst layer consistently. In addition,

### INTRODUCTION

The Polymer Electrolyte Fuel Cell (PEFC) has gained popularity recently and is being used in various industries, including the automobile industry, stationary power production, and others. This is due to advancements in electrode catalyst properties and membrane technology. However, in order to make fuel cell devices more widely available to consumers, a further drop in cost is highly recommended. There are numerous ways to lower the price of the PEFC component. PEFC's water management is one of them [1]. Generally speaking, even while a humidifier is necessary for PEFC operation in order to prevent membrane drying, using one results in lower system efficiency and higher overall PEFC system costs. Additionally, it results in the flooding and clogging phenomena.

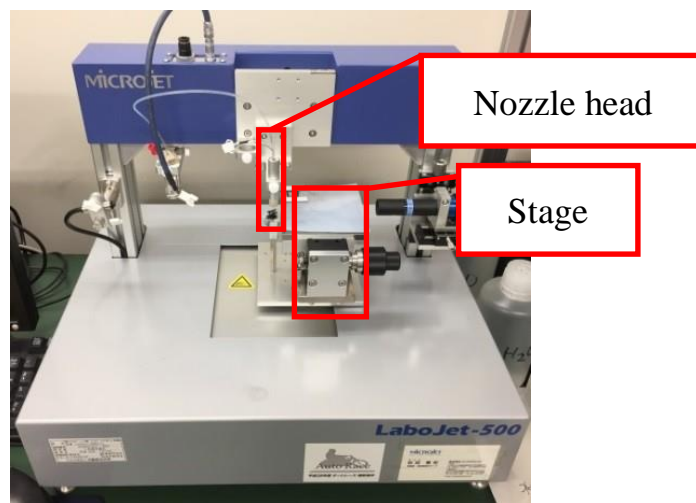


**Figure 1.** Photograph of inkjet coating printer

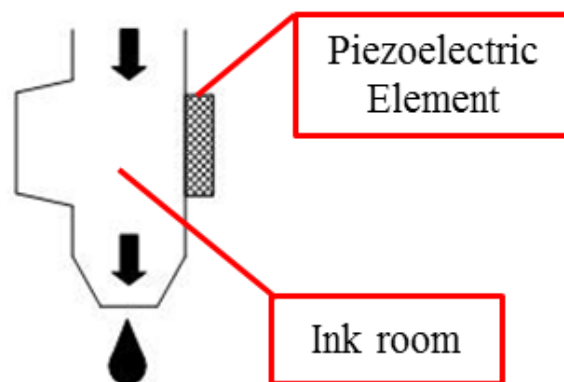


**Figure 2.** Schematic diagram of nozzle head

## EXPERIMENT

### Inkjet coating printer

Labojet-500 made by MICROJET Corporation was adopted for our work printing the catalyst layer. The inkjet coating printer can discharge Pt catalyst ink continuously from the nozzle head of 80 $\mu$ m diameter. In addition, because the x axis and y axis of the stage are controlled by a computer, we can also print the catalyst layer of complex shape. A discharging method of the inkjet coating printer is adopted piezoelectric discharge technology as shown in Figure 2. The nozzle head has an ink room that stores Pt ink, and the piezoelectric element. The ink exhaled by the expansion of piezoelectric element, and it is supplied to the ink room from a ink tank by shrinking the piezoelectric element. Here, the feature of this discharging technology is that there is no influence on ink by heating and it is to be able to use various inks.

### Method of preparing catalyst ink

Firstly, the catalyst slurry for the doctor blade method as shown in Table 1 was applied to the inkjet coating printer as the catalyst ink. However, because the slurry with a high viscosity blocked the nozzle head, it was not able to be discharged by inkjet coating printer. Therefore, the slurry has been improved as the catalyst ink by adding a solvent and water to control the viscosity appropriately as shown in Table 1. Although the improved ink was able to be coated onto the membrane using the inkjet coating printer, the catalyst layer became like spots, and the thickness was a heterogeneous as shown in Figure 3 (a). The carbon supports used at Pt catalyst was agglomerated into the catalyst ink. Therefore, we applied the distributed processing to the catalyst ink to disperse the agglomerated carbon supports.

The catalyst ink was dispersed by using an ultrasonic wave crusher and a vacuum stirring mill. As a result, the catalyst layer was formed uniformly by applying the distributed processing mentioned above as shown in Figure 3 (b).

### Printing program to manufacture catalyst layer

In order to print a catalyst layer, we prepared two different printing programs that called Inkjet-A and Inkjet-B. Inkjet- A was programmed so that Pt catalyst ink was exhaled every 100 $\mu\text{m}$  according to x axis and y axis by in-line arrangement as shown in Figure 4 (a). On the other hand, Inkjet-B was programmed so that Pt catalyst ink was exhaled every 100 $\mu\text{m}$  according to x axis and y axis by staggered arrangement as shown in Figure 4 (b). Here, Inkjet-B was exhaled four times as shown in Figure 4 (b) to match the catalytic amount of each application pattern. Figure 5 shows the SEM images of catalyst layer surface printed by each application pattern. Although the nozzle hole diameter is 80 $\mu\text{m}$  and the gap between each dot is 20 $\mu\text{m}$ , the surface coated by Inkjet-A is smooth as shown in Figure 5 (a). This reason is that the exhaled droplet extends on the Teflon<sup>®</sup> sheet, consequently the adjoined droplet unites according to the surface tension. On the other hand, the surface coated by Inkjet-B has some pinholes as shown in Figure 5 (b). Because the droplet exhaled by each printing process is dried instantaneously and the gap of each dot is longer than that of Inkjet- A, the adjoined droplet is not able to unite and the surface has some pinholes. We also examined the influence of these pinholes in the catalyst layer on the cell performance to establish the manufacturing method of the catalyst layer using the ink jet coating printer.

### Experimental apparatus and method

Figure 6 shows the structure of 9cm<sup>2</sup> of PEFC single cell [4]. The catalytic layer of 1cm<sup>2</sup> was pressed onto the midrange of the membrane of 9cm<sup>2</sup> by a hot press. Both separators were made of carbon, and have a serpentine gas channel of 1mm $\times$ 1mm. Figure 7 shows the experimental apparatus for the evaluation of the cell performance. Anode gas and cathode gas were humidified by passing through the humidifier and were supplied to the cell. In order to prevent dew formation in the supply pipe, the piping between the humidifier and the cell was made shorter, and the piping temperature was maintained at 80 $^{\circ}\text{C}$  by a ribbon heater. The cell performance was measured by the fuel cell impedance meter (KIKUSUI KFM2005), was evaluated by IV characteristics and impedance characteristics.

**Table 1.** Properties of catalyst slurry and catalyst ink

Item	Quantity	
	catalys t slurry	catalys tink
Pt catalyst (TEC10V40E) [g]	0.5	0.5
Purified water[ml]	1.0	7.0
Ethanol[ml]	0.5	3.5
20%Nafion <sup>®</sup> dispersion solution [ml]	1.5	1.5



(a)After adding solvent      (b) After dispersion processing

**Figure 3.** Optimization of catalyst ink for printing process

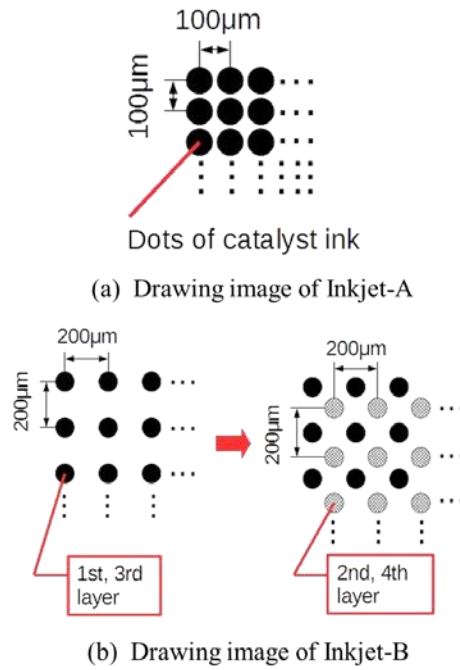
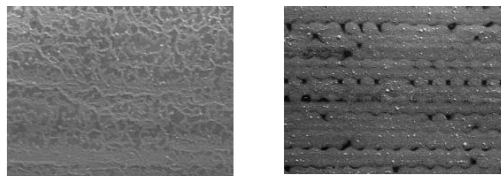


**Figure 4.** Both printing patterns



(a) SEM image of Inkjet-A (b) SEM image of Inkjet-B

**Figure 5.** SEM images of the surface of the catalyst layer coated by each printing pattern

The experimental conditions were two humidifying conditions as shown in Table 2. The standard condition means the full humidifying whose all temperature were 80°C. The advanced condition means that both supplied gas was not humidified, and the cell temperature was not heated by a heater plate and was maintained at room temperature. The current density was 0.4A/cm<sup>2</sup>, the fuel gas utilization was 70%, and the oxidant gas utilization was 40%, respectively. The operating pressure was atmospheric. Here, because both gas utilizations were calculated as Eq.(1) and (2) by the current density of 0.4A/cm<sup>2</sup>, each gas shifts to the condition of depletion if the current density exceeds 0.4A/cm<sup>2</sup> [5,6].

$$\text{Fuel Utilization} = \frac{i \times A \times n \times \frac{22.4}{T}}{2 \times F \times \dot{Q}_{H_2}} \quad (1)$$

$i$  [A/cm<sup>2</sup>] : current density,  $A$  [cm<sup>2</sup>] : electrode area,  
 $n$  : number of cells,  $T$  [K] : normal temperature,  $T_0$  [K] : operation temperature,  $\dot{Q}_{H_2}$  [ml/min] : flow rate of  $H_2$  gas,  $F$  : Faraday constant

$$\text{Air Utilization} = \frac{i \times A \times n \times \frac{22.4}{T}}{4 \times F \times \dot{Q}_{O_2}} \quad (2)$$

$Q_{Air}$  [ml/min] : flow rate of Air gas

**Table 2.** Experimental conditions

	Standard	Advanced
Fuel Utilization		70%
Air Utilization		40%
Current Density		0.4 A/cm <sup>2</sup>
Cell Temperature	80°C	Room temperature : About 25 –27°C
Humidifier Temperature (AN)	80°C	Not use
Humidifier Temperature (CA)	80°C	Not use

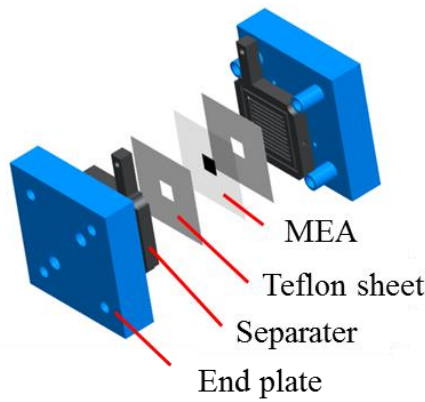


**Figure 6.** PEFC cell structure

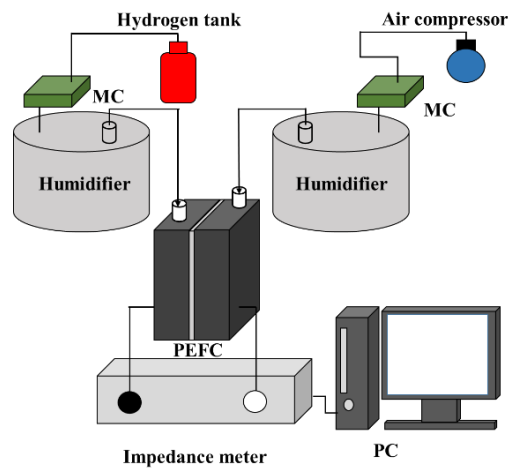


**Figure 7.** Schematic diagram of experimental apparatus

As an AC impedance measurement condition, a frequency range was from 10,000 to 0.07Hz, and superimposed currents were 0.2A and 0.4A, respectively. Here, although the Cole-Cole plots should be

measured under the current density of 1A/cm<sup>2</sup> or more to confirm the influence of the diffusion polarization, the Cole-Cole plots in a high current region was measured under 0.4A/cm<sup>2</sup> to compare all cells.

## RESULTS AND DISCUSSIONS

Evaluate of the cell performance at the different manufacturing methods

The cell performance of the new MEA manufactured by the inkjet coating printer is evaluated under two experimental conditions by comparing with the conventional MEA manufactured by doctor blade method. Figure 8 shows the comparison of two coating method on I-V performance under two experimental conditions. Here, the cell voltage is shown as IR free. At standard condition, the cell voltage of the new MEA is better than the conventional MEA in all current density regions. Although the cell with the new MEA was able to generate electricity until 0.85A/cm<sup>2</sup> of a current density, the cell with the conventional MEA was able to generate electricity only until 0.5A/cm<sup>2</sup>. Figure 9 shows the comparison of two coating method on Cole-Cole plots at 0.4A/cm<sup>2</sup> under two experimental conditions. The Cole- Cole plots is emanated in a low frequency region under the standard condition though it is converged under the advanced

condition. Generally, because the emanation of the circular arc by the low frequency region means growing the diffusion polarization, the cell with the MEA made by the doctor blade caused the flooding phenomenon at 0.4 A/cm<sup>2</sup>.

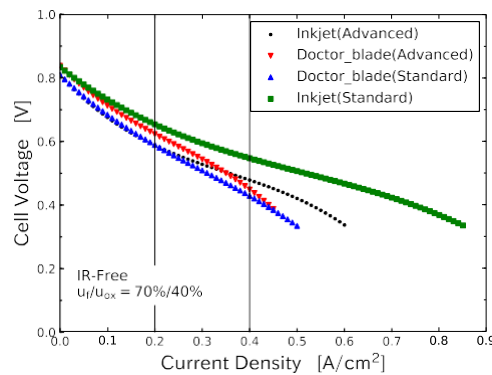


**Figure 8.** Comparison of two coating method on I-V performance

The resistance polarization of the new MEA with about 323m $\Omega$  is smaller than the conventional MEA with about 560m $\Omega$ . Although the activation polarization of the new MEA is about 412m $\Omega$ , that of the conventional MEA was not able to be obtained because the Cole-Cole plot was not convergent. This reason is elucidated by SEM image of cross section as shown in Figure10. From the SEM image, the thickness of the catalyst layer is from 1.94 to 5.28 $\mu$ m. On the other hand, because the general thickness of the catalyst layer manufactured by doctor blade method in our laboratory is about 30 $\mu$ m, the new one is 5 - 6 times thinner than the conventional one. An increase of three phase interface as a reaction field is enhanced by the thin catalyst layer, an improvement of a gas diffusion and a control of a flooding phenomena. That is, ununiformed catalyst layer as shown in Fig.10 increases an effective electrode area, and the thin catalyst layer makes reaction gas easily reach the Pt catalyst, and water generated by the cell reaction also drains easily to outside the catalyst layer. The decreasing rate of the catalytic layer thickness of a conventional MEA and an inkjet MEA was estimated to verify this guess. However, because a conventional MEA is too thick, it is not possible to cut it by the ion milling normally and consequently the cross section of a conventional MEA was not able to be measured by a SEM. Therefore, because an electrode thickness is assumed to be corresponding to an internal resistance, we estimated the decreasing rate of the catalytic layer thickness by calculating the equation as follows;

A resistance of a new MEA  $R_{IJ}$  [ $\Omega$ ] is expressed as follows, and a thickness of a new MEA  $t_{IJ}$  [m] is expressed as Eq. (3).

$$R_{IJ} = \rho \frac{t_{IJ}}{A} \text{ therefore } t_{IJ} = \frac{0.323 A}{\rho} \quad (3)$$

Here,  $A$  [ $m^2$ ] means an electrode area,  $\rho$  [ $\Omega m$ ] means an electrical resistivity, respectively. To similar, a thickness of a conventional MEA  $t_{DB}$  [ $m$ ] is expressed as Eq.(4).

$$R_{DB} = \rho \frac{t_{DB}}{A} \text{ therefore } t_{DB} = \frac{0.560 A}{\rho} \quad (4)$$

Here, because an electrode area of each MEA is same, and each catalyst layer is made of similar catalyst ink, it is assumed that both electrical resistivities are also same. Consequently, the decreasing rate of the catalytic layer thickness is calculated as follow.

$$\frac{t_{DB} - t_{IJ}}{t_{DB}} = \frac{0.560 - 0.323}{0.560} = 0.42 \quad (5)$$

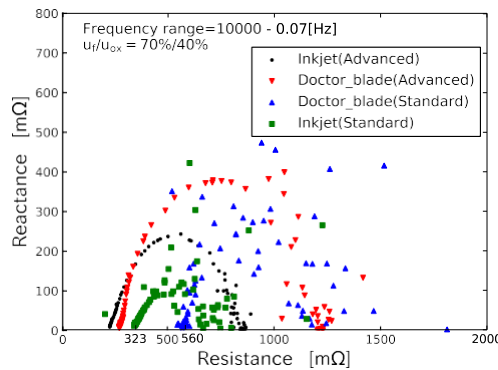


**Figure 9.** Comparison of difference method on Cole-Cole plot at  $0.4A/cm^2$  of current density

From the calculation result, because the decreasing rate of the catalytic layer thickness is about 42%, the catalyst layer made by an inkjet coating printer was able to be reduced about 42% of Pt catalyst compared with the one made by doctor blade method if Pt catalyst was dispersed in the catalyst layer uniformly. To verify this assumption, the amount of Pt of each MEA was analyzed by a thermogravimetric analysis. From this analysis result, the amount of Pt catalyst of the MEA made by doctor blade method is  $671\mu g/cm^2$ , and the one made by an inkjet coating printer is  $425\mu g/cm^2$ . Therefore, the Pt catalyst reduction rate becomes about 37%. This result is almost the same as the decreasing rate of the catalytic layer. The difference between the two results originates in the ununiformity dispersion of Pt in a catalyst layer.

On the advanced experimental condition (w/o heating/ humidifying), the cell voltage of the new MEA is worse than the conventional MEA in a low current density region. However, it reverses when the current density exceeds  $0.35A/cm^2$  as shown in Figure 8. Furthermore, the resistance and activation polarizations of the new MEA are about  $50m\Omega$  and  $300m\Omega$  smaller than that of the conventional MEA respectively as shown in Figure9. Generally, because the membrane keeps a good proton conductivity by wetting, the Nafion® solution has been added to the catalyst layer as an ionomer. Therefore, the activation polarization under the advanced condition becomes larger than that under the standard condition because the three phase interface decreases by which dry-ionomer in the catalyst layer cannot transport proton. Moreover, the conventional MEA of this tendency is larger than that of the new MEA because the conventional MEA with thick catalyst layer that has more ionomers needs more water. In a low current density region, the cell performance of the new MEA becomes bad because the supplied dry gas deprives of moisture in the thin catalyst layer easily. In a high current density region, as the drying and the wet equiponderate, the cell performance is enhanced. Because the catalyst layer of the conventional MEA is thick, the evaporation of moisture in the catalyst layer with the dry gas becomes slow because of a large amount of storage water. Here, the cell performance of the conventional MEA under the standard condition looks worse than that under the advanced condition because the I-V curve as shown in Fig.8 is expressed as the IR Free. The



resistance under the advanced condition when the I-V characteristic was measured was 100mΩ higher than that under the standard condition. Moreover, because the resistance under the advanced condition decreased gradually with the increase of a current density, the decrease rate of the IR-Free of MEA under the advanced condition grows in the high current density region. Therefore, under the advanced condition, the resistance polarization greatly depends on the amount of water produced by the cell reaction, and this tendency of a conventional MEA with a thick catalyst layer as a large water storage tank is larger than that of a new MEA.

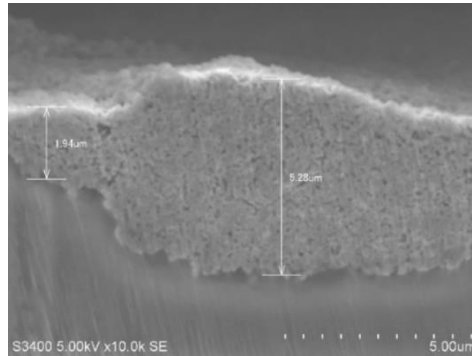


**Figure 10.** SEM image of new catalyst layer

To confirm the influence of the water generated at the cathode side, we compare the Cole-Cole plot that measured at

0.2 and 0.4[A/cm<sup>2</sup>] under the advanced condition as shown in Figure 11. Although the activation polarization of the new MEA at 0.4A/cm<sup>2</sup> is 625mΩ, it is 712mΩ at 0.2A/cm<sup>2</sup>. It is clarified that the activation polarization of the new

MEA is decreased by water generated by the cell reaction. Our hypothesis was proven to be correct. On the other hand, in conventional MEA, both the activation polarizations at different current density are about equal as shown in Figure

12. Because the thickness of the catalyst layer in conventional MEA is 5 - 6 times larger than the new catalyst layer, the water generated with 0.4A/cm<sup>2</sup> in current density doesn't arrive to wet the ionomer in the catalyst layer enough, and it does not also make three phase interfaces increase.

From the mention above, we confirmed that the performance of the MEA manufactured by the inkjet coating printer is improved compared to the conventional MEA using the doctor blade method at both experimental conditions. In addition, because the new MEA demonstrates the performance more in a high current density region under the advanced condition, it is expected to reduce the costs of Pt catalyst and the system without a humidifier.

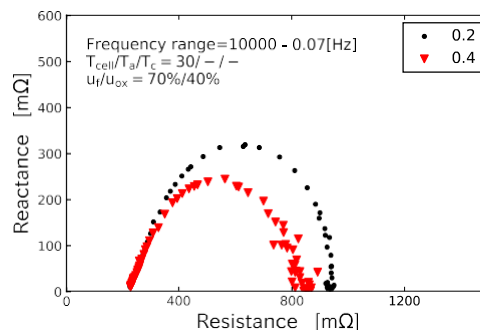


**Figure 11.** Influence of current density on Cole-Cole plot of the new MEA

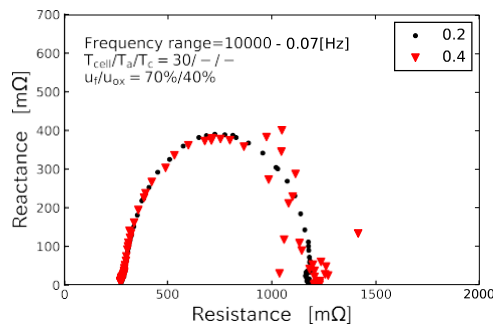


**Figure 12.** Influence of current density on Cole-Cole plot of the

conventional MEA Influence of catalyst layer structure on the cell performance

Generally, an inkjet coating printer can print various structures of the catalyst layer. We also examined the influence of the catalyst layer structure as shown in Figure 5 on the cell performance. Here, the cell performance was evaluated under the advanced condition. Figure 13 shows the comparison of I-V performance between the MEA-A and the MEA- B patterns. Although both of OCVs are almost same, the I-V performance of MEA-A better than that of MEA-B clearly. Especially, though the cell voltage of MEA-B improves a little with the increase of water produced by the cell reaction, it decreases drastically by increasing the diffusion polarization when the current density exceeds about 0.3A/cm<sup>2</sup>. From the Cole-Cole plots shown in Figure 14, because the Cole-Cole plots of MEA-B is larger than that of MEA-A clearly, the activation poralization is larger. Moreover, the resistance polarization of MEA-B is about twice as large as MEA-

A. Therefore, the decline of the cell performance of MEA-B originates in the pinholes in the catalyst layer. In a low current density region with less generated water, the supplied dry gas reaches to the membrane through the pinholes directly, consequently the transport of proton from anode side to cathode side is disturbed because of drying of ionomer in the catalyst layer. On the other hand, in a high current density region, the reactant gas such as hydrogen and oxygen were not able to reach to Pt catalyst by which water generated by the cell reaction collect in the pinholes of the catalyst layer and it causes the flooding phenomenon by penetrating into GDL. Consequently, we confirmed that the existence of the pinholes in the catalyst layer causes the degradation of the cell performance. However, Dr. A. Scott et al reported that an initial cell performance was enhanced if the catalyst layer had the defects like pinholes. On the other hand, they also mentioned that because this defect gradually damaged a membrane, consequently the life performance of the cell was deteriorated [7]. Therefore, because the defect during the applying process of a catalyst layer has to be removed, the coating method without the pinholes should be optimized as future works [8-11].

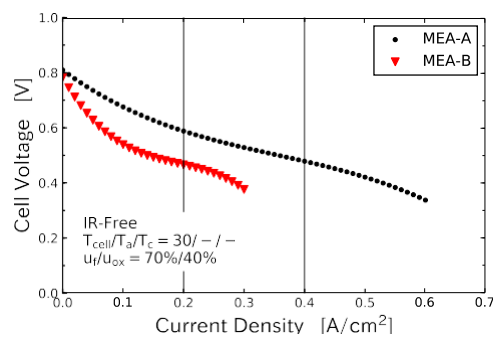


**Figure 13.** Comparison of difference catalyst layer structure with I-V performance

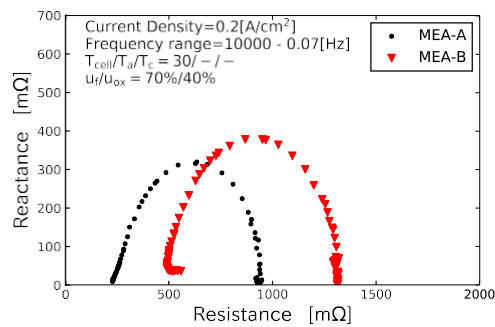


**Figure 14.** Comparison of difference catalyst layer structure with Cole-Cole plot at

$0.2\text{A}/\text{cm}^2$

## CONCLUSIONS

The objective of the study is “Evaluation of PEFC cell performance of MEA using the catalyst layer manufactured by inkjet coating printer”. The results obtained in this study are summarized as follows below.

- We were able to confirm that the catalyst ink can exhale from the inkjet printer by preparing the catalyst ink that the viscosity is adjusted for the inkjet printer. In addition, the distributed process is necessary to form the catalyst layer where Pt is uniformly dispersed.
- The cell performance of the MEA manufactured by the inkjet coating printer is enhanced compared with the conventional MEA using doctor blade method because the thickness of the catalyst layer of the new MEA is 5 – 6 times thinner than the conventional MEA.
- Because the cell performance of the new MEA is better than the conventional MEA even if neither humidifying the supplied gas nor heating of the cell, we can expect the reduction of PEFCs system costs.
- Because we confirmed that the existence of the pinholes in the catalyst layer causes the degradation of the cell performance, the coating method without the pinholes should be optimized as future works.

## ACKNOWLEDGEMENTS

This work was supported by JKA and its promotion funds from AUTO RACE

(2017M-116).

## REFERENCES

- [1] K. Sugiura, N. Takahashi, T. Kamimura. “New design of a PEFC cathode separator of for water management”. IOP Conf. Series: *Earth and Environmental Science*, vol. 93, 012017, 2017.
- [2] I. Ota, K. Sugiura, T. Ito, K. Inukai, M. Utaka. “Development of MEA with self-water management on PEFC to reduce the manufacturing cost”. *ECS Transactions*, vol. 83, no. 1, pp. 23-29, 2018.
- [3] M. Usman, N. Badshah, F. Ghaffar. “Higher Order Compact Finite Difference Method For The Solution Of 2-D Time Fractional Diffusion Equation”. *Matrix Science Mathematic*, vol. 1, no. 1, pp. 04-08, 2018.
- [4] L. Xu. “Research on Anti-Overtuning Performance Of Multi-Span Curved Girder Bridge with Small Radius”. *Acta Mechanica Malaysia*, vol. 1, no. 1, pp. 04-07, 2018.
- [5] B.Q. Li, Z. Li. “Design of Automatic Monitoring System for Transfusion”. *Acta Electronica Malaysia*, vol. 2, no. 1, pp. 07-10, 2018.

- [6] X.G. Yue, M.A. Ashraf. “Opposite Degree Computation and Its Application”. *Engineering Heritage Journal*, vol. 2, no. 1, pp. 05-13, 2018.
- [7] A.D. Taylor , E.Y. Kim, V.P. Humes, J. Kizuka, L. T. Thompson. “Inkjet printing of carbon supported platinum 3-D catalyst layers for use in fuel cells”. *Journal of Power Sources*, vol. 171, pp. 101–106, 2007.
- [8] F. Okazaki, K. Sugiura, T. Ito, K. Inukai, M. Utaka. “Selection of the Optimized Carbon Material for PEFC Separator”. *ECS Transactions*, vol. 83, no. 1, pp. 45-51, 2018.
- [9] R. Arai, K. Sugiura, M. Yamauchi. “Development of Catalyst Layer with Self-water Management for PEFC”. *ECS Transactions*, vol. 65, no. 1, pp. 129-135, 2015.
- [10] Y. Matsumoto, K. Sugiura. “Establishment of performance diagnostics for PEFC stack”. *ECS Transactions*, vol. 65, no. 1, pp. 183-189, 2015.
- [11] S.A. Mauger, K. C. Neyerlin, A. C. Yang-Neyerlin, K.L. More, M. Ulsh. “Gravure Coating for Roll-to-Roll Manufacturing of Proton-Exchange-Membrane Fuel Cell Catalyst Layers”. *J. Electrochem. Soc.*, vol. 165, no. 11, F1012-F1018, 2018.